

# Electrodisintegration of ${}^3\text{He}$ below and above deuteron breakup threshold

L.E. Marcucci<sup>1,2</sup>, M. Viviani<sup>2,1</sup>, R. Schiavilla<sup>3,4</sup>, A.Kievsky<sup>2,1</sup>, and S. Rosati<sup>1,2</sup>

<sup>1</sup> Department of Physics, University of Pisa, I-56100 Pisa, Italy

<sup>2</sup> INFN, Sezione di Pisa, I-56100 Pisa, Italy

<sup>3</sup> Department of Physics, Old Dominion University, Norfolk, Virginia 23529, USA

<sup>4</sup> Jefferson Lab, Newport News, Virginia 23606, USA

Received: 20 September 2004 / Published Online: 8 February 2005

© Società Italiana di Fisica / Springer-Verlag 2005

**Abstract.** Recent advances in the study of electrodisintegration of  ${}^3\text{He}$  are here presented and discussed. The pair-correlated hyperspherical harmonics method is used to calculate the initial and final state wave functions, with a realistic Hamiltonian consisting of the Argonne  $v_{18}$  two-nucleon and Urbana IX three-nucleon interactions. The model for the nuclear current and charge operators retains one- and many-body contributions. Particular attention is made in the construction of the two-body current operators arising from the momentum-dependent part of the two-nucleon interaction. Three-body current operators are also included so that the full current operator is strictly conserved. The present model for the nuclear current operator is tested comparing theoretical predictions and experimental data of  $pd$  radiative capture cross section and spin observables.

**PACS.** 21.45.+v Few-body systems – 25.10.+s Nuclear reactions involving few-nucleon systems – 25.30.Dh Inelastic electron scattering to specific states – 25.30.Fj Inelastic electron scattering to continuum – 25.40.Lw Radiative capture

## 1 Introduction

The theoretical study of the electromagnetic structure of few-body nuclei requires the knowledge of the nuclear wave functions and electromagnetic transition operators. In the case of processes involving two and/or three nucleons, it is possible to obtain very accurate bound- and scattering-state wave functions from realistic Hamiltonian models. Therefore, the different models for the nuclear electromagnetic current operator can be tested with the large variety of electromagnetic observables involving  $A=2$  and 3 nuclei. In particular, we concentrate our attention on the  $pd$  radiative capture and on the electrodisintegration of  ${}^3\text{He}$  below and above deuteron breakup threshold (DBT). These processes have been extensively studied by several research groups (see [1] for a review). Most recently, the  $pd$  radiative capture and the  ${}^3\text{He}(e, e')$  reactions below DBT have been investigated by our group in [2]. The pair-correlated hyperspherical harmonics (PHH) method [3] has been used to calculate the  $A=3$  bound- and scattering-state wave functions from a realistic Hamiltonian model consisting of the Argonne  $v_{18}$  two-nucleon [4] and Urbana IX three-nucleon [5] interactions (AV18/UIX). The nuclear electromagnetic current operator included, in addition to the one-body convection and spin-magnetization terms, also two-body contributions. These two-body terms were constructed follow-

ing the method of [6], with the goal of satisfying the current conservation relation (CCR) with the AV18. However, within this method, only the dominant two-body terms, constructed from the momentum-independent part of the AV18, satisfy the CCR with this part of the interaction [7]. The two-body terms originated from the momentum-dependent part of the AV18 are not strictly conserved. In [2], further transverse contribution, associated with the  $\rho\pi\gamma$  and  $\omega\pi\gamma$  transition mechanisms and with the excitation of intermediate  $\Delta$  resonances, were included.

The main conclusions of [2] can be summarized as follows: the two-body contributions to the electromagnetic charge and current operators are crucial to achieve an overall good agreement between theory and experiment for all the observables under investigation. However, some discrepancies between theory and experiment have been found, in particular for the deuteron tensor polarization observables  $T_{20}$  and  $T_{21}$  of  $pd$  radiative capture at center-of-mass energy  $E_{c.m.} = 2$  MeV, and, in [8], also at  $E_{c.m.} = 3.33$  MeV. In the analysis of [2] it has been suggested that these discrepancies might be due to the fact that the electromagnetic current operator satisfies only approximately the CCR with the used nuclear Hamiltonian. In fact, when the  $T_{20}$  and  $T_{21}$  observables are calculated in the long-wavelength approximation (LWA), ap-

plying the Siegert theorem, a quite good agreement with the data is obtained.

In this work we present a new model for the nuclear current operator which *exactly* satisfies the CCR with the AV18/UIX Hamiltonian model. The model is then tested in the study of the  $pd$  radiative capture at the two previously considered values of  $E_{c.m.}$ , 2 and 3.33 MeV, and in the study of inclusive and exclusive electrodisintegration of  ${}^3\text{He}$ , both below and above DBT. The model for the nuclear electromagnetic current and charge operators is summarized in the following section. A detailed review will be given elsewhere [9]. Finally, the theoretical results are compared with the experimental data in Sect. 3.

## 2 The nuclear electromagnetic charge and current operators

The nuclear electromagnetic charge  $\rho(\mathbf{q})$  and current  $\mathbf{j}(\mathbf{q})$  operators can be written as sums of one- and many-body terms that operate on the nucleon degrees of freedom. The one-body operators  $\rho_i(\mathbf{q})$  and  $\mathbf{j}_i(\mathbf{q})$  for particle  $i$  are derived from the non-relativistic reduction of the covariant single-nucleon current, by expanding in powers of  $1/m$ ,  $m$  being the nucleon mass [1]. The model commonly used [10] for the two-body charge operators includes the  $\pi$ -,  $\rho$ -, and  $\omega$ -meson exchange terms with both isoscalar and isovector components, as well as the (isoscalar)  $\rho\pi\gamma$  and (isovector)  $\omega\pi\gamma$  charge transition couplings. At moderate values of momentum transfer ( $q < 5 \text{ fm}^{-1}$ ), the  $\pi$ -meson exchange charge operator has been found to give the dominant two-body contribution [11].

The electromagnetic current operator must satisfy the CCR, written as

$$\mathbf{q} \cdot \mathbf{j}(\mathbf{q}) = [H, \rho(\mathbf{q})], \quad (1)$$

where the nuclear Hamiltonian  $H$  is taken to consist of two- and three-body interactions, denoted as  $v_{ij}$  and  $V_{ijk}$  respectively. To lowest order in  $1/m$ , (1) separates into

$$\mathbf{q} \cdot \mathbf{j}_i(\mathbf{q}) = \left[ \frac{\mathbf{p}_i^2}{2m}, \rho_i(\mathbf{q}) \right], \quad (2)$$

$$\mathbf{q} \cdot \mathbf{j}_{ij}(\mathbf{q}) = [v_{ij}, \rho_i(\mathbf{q}) + \rho_j(\mathbf{q})], \quad (3)$$

and similarly for the three-body current  $\mathbf{j}_{ijk}(\mathbf{q})$ . We have neglected the two-body terms in  $\rho(\mathbf{q})$ , which are of order  $1/m^2$ . The one-body current is easily shown to satisfy (2). To construct the two-body current, it is useful to adopt the classification scheme of [12], and separate the current  $\mathbf{j}_{ij}(\mathbf{q})$  into model-independent (MI) and model-dependent (MD) parts. The MI two-body current has a longitudinal component and is constructed so as to satisfy the CCR of (3), while the MD two-body current is purely transverse and therefore is un-constrained by the CCR. The latter is taken to consist of the isoscalar  $\rho\pi\gamma$  and isovector  $\omega\pi\gamma$  transition currents, as well as the isovector current associated with excitation of intermediate  $\Delta$  resonances as in [2].

The MI two-body currents arising from the momentum-independent terms of the AV18 two-nucleon interaction have been constructed following the standard procedure of [6], which will be hereafter quoted as meson-exchange (ME) scheme. It can be shown that these two-body current operators satisfy *exactly* the CCR with the first six operators of the AV18. The two-body currents arising from the spin-orbit components of the AV18 could be constructed using again ME mechanisms [13], but the resulting currents turn out to be not strictly conserved. The same can be said of those currents deriving from the quadratic momentum-dependent components of the AV18, if obtained, as in [2], by gauging only the momentum operators, but ignoring the implicit momentum dependence which comes through the isospin exchange operator (see below). Since our goal is to construct MI two-body currents which satisfy *exactly* the CCR of (3), the currents arising from the momentum-dependent terms of the AV18 interaction have been obtained following the procedure of [14], which will be quoted as minimal-substitution (MS) scheme. The main idea of this procedure, fully reviewed and extended in [9], is that the isospin operator  $\tau_i \cdot \tau_j$ , which gives the isospin-dependence of the isospin-conserving part of all realistic two-nucleon interactions, is formally equivalent to an implicit momentum dependence [14]. In fact,  $\tau_i \cdot \tau_j$  can be expressed in terms of the space-exchange operator,  $P_{ij} = e^{\mathbf{r}_{ji} \cdot \nabla_i + \mathbf{r}_{ij} \cdot \nabla_j}$ , using the formula

$$\tau_i \cdot \tau_j = -1 - (1 + \sigma_i \cdot \sigma_j) P_{ij}, \quad (4)$$

valid when operating on antisymmetric wave functions. In the presence of an electromagnetic field, minimal substitution is performed both in the momentum dependent terms of the two-nucleon interaction and in the space-exchange operator  $P_{ij}$  of (4), and the resulting current operators are then obtained with standard procedures [9,14]. Explicit formulas can be found in [9]. Here we only quote the result for the currents arising from the momentum-independent part of the AV18 interaction ( $v_{ij}^0$ ):

$$\mathbf{j}_{ij}(\mathbf{q}) = i v_{ij}^0 \left( \epsilon_i \int_{\gamma_{ij}} ds e^{i\mathbf{q} \cdot \mathbf{s}} + \epsilon_j \int_{\gamma'_{ji}} ds' e^{i\mathbf{q} \cdot \mathbf{s}'} \right) (1 + \tau_i \cdot \tau_j), \quad (5)$$

where  $\epsilon_i$  is the nucleon charge operator, and  $ds$  ( $ds'$ ) is the infinitesimal step on the generic path  $\gamma_{ij}$  ( $\gamma'_{ji}$ ) that goes from position  $i$  ( $j$ ) to position  $j$  ( $i$ ). Two observations are in order: (i) with a particular choice of the integration path it is possible to re-obtain the two-body current operators calculated, within the ME scheme, from the momentum-independent part of the AV18 [9]; (ii) in the limit  $\mathbf{q} \rightarrow 0$ , the current operator  $\mathbf{j}_{ij}(\mathbf{q})$  of (5) becomes path-independent and unique. To simplify the calculation, the integration paths  $\gamma_{ij}$  and  $\gamma'_{ji}$  have been chosen to be linear.

Both the ME and the MS schemes can be generalized to calculate the three-body current operators induced by the three-nucleon interaction (TNI)  $V_{ijk}$ . Here, these three-body currents have been constructed within the ME scheme to satisfy the CCR with the Urbana-IX TNI [5].

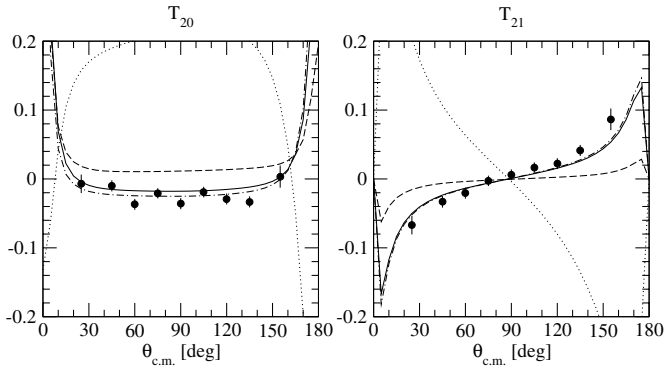


**Fig. 1.** Deuteron tensor polarization observables  $T_{20}$  and  $T_{21}$  for  $pd$  radiative capture at  $E_{c.m.} = 2$  MeV, obtained with the AV18 Hamiltonian models. See text for explanations of the different curves. The experimental data are from [19]

However, the same procedure can be applied to other models of TNI's, such as the Tucson-Melbourne [15] and Brazil [16] models. Details of the calculation can be found in [9].

In summary, the present model for the many-body current operator retains the two-body terms obtained within the ME scheme from the momentum-independent part of the AV18, those ones obtained within the MS scheme from the momentum-dependent part of the AV18, the MD terms quoted above, and the three-body terms obtained within the ME scheme from the UIX. Thus, the full current operator satisfies *exactly* the CCR with the AV18/UIX nuclear Hamiltonian. In contrast, the model of [2] retains only two-body currents, all of them obtained within the ME scheme.

### 3 Results

In the present section we compare the theoretical prediction and experimental data for two sets of  $^3\text{He}$  electrodisintegration observables: (i) the longitudinal and transverse response functions  $R_L$  and  $R_T$  for  $^3\text{He}(e, e')$  at momentum transfer values  $q = 0.88, 1.64$  and  $2.47 \text{ fm}^{-1}$  and excitation energies ( $E_x$ ) from two-body threshold up to 20 MeV; (ii) the differential cross section of the  $^3\text{He}(e, e')p$  reaction as function of the missing momentum in  $(q, \omega)$ -constant kinematics, at beam energies of 370 and 576 MeV and  $q$  values of 412, 504 and 604 MeV/c. Data are respectively from [17] and [18].

However, preliminarily, we report some results for the  $pd$  radiative capture reaction, to show that the new model for the many-body nuclear current operators resolves some of the discrepancies between theory and experiment of [2]. The  $T_{20}$  and  $T_{21}$  observables at  $E_{c.m.} = 2$  MeV using the AV18 two-nucleon interaction are shown in Fig. 1. The dotted curves are obtained including only the one-body current contributions, the dashed curves are obtained with the model for the nuclear current operator of [2], and the dotted-dashed curves are obtained in the long-wavelength-approximation (LWA), applying the Siegert theorem. Finally, the solid curves are obtained including the one- and

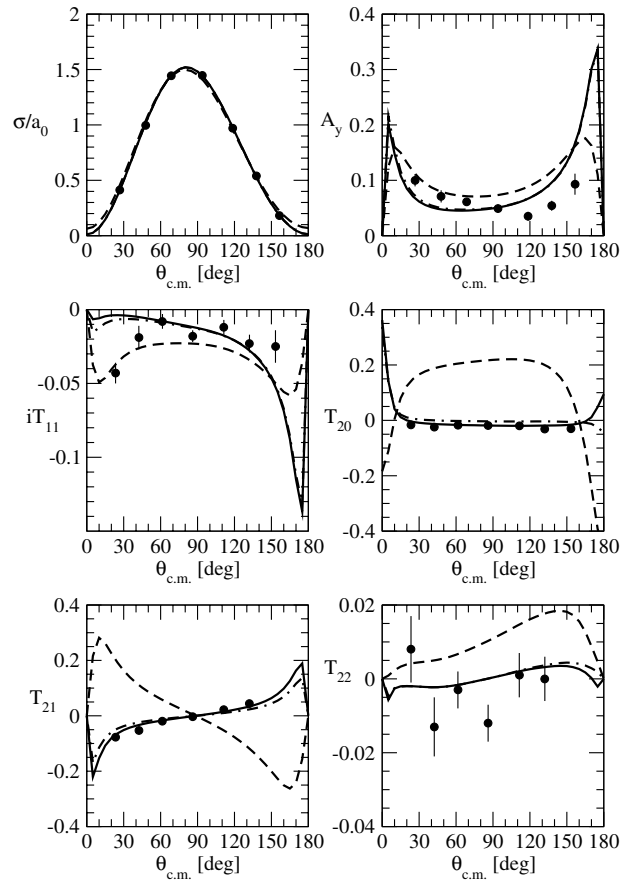


**Fig. 2.** Differential cross section, proton vector analyzing power, and the four deuteron tensor polarization observables for  $pd$  radiative capture at  $E_{c.m.} = 3.33$  MeV, obtained with the AV18/UIX Hamiltonian model. See text for the explanations of the different curves. The experimental data are from [20]

two-body contributions described in Sect. 2, necessary to satisfy the CCR with the AV18 nuclear Hamiltonian. Data are from [19]. By inspection of Fig. 1, we observe that there is a good agreement between the experimental data, the LWA and the present “full” results, while the results of [2] are in disagreement, as expected, with both the LWA and experimental results. The excellent agreement between the LWA and the “full” results is a consequence of the fact that the “full” nuclear electromagnetic current operator satisfies the CCR with the AV18 nuclear Hamiltonian.

As an example of the degree of agreement which has been reached between the present calculation and experimental data for the  $pd$  radiative capture, we show in Fig. 2 the theoretical predictions obtained with the AV18/UIX Hamiltonian model at  $E_{c.m.} = 3.33$  MeV. Data are from [20]. The dashed, dotted-dashed and solid curves correspond to the calculation with one-body only, with one- and two-body, and with one-, two- and three-body currents. An overall nice description has been reached for all the observables, with the only exception of the  $iT_{11}$  deuteron polarization observable at small angles. Also, some small three-body currents effects are noticeable, especially in the  $T_{20}$  and  $T_{21}$  deuteron tensor observables,

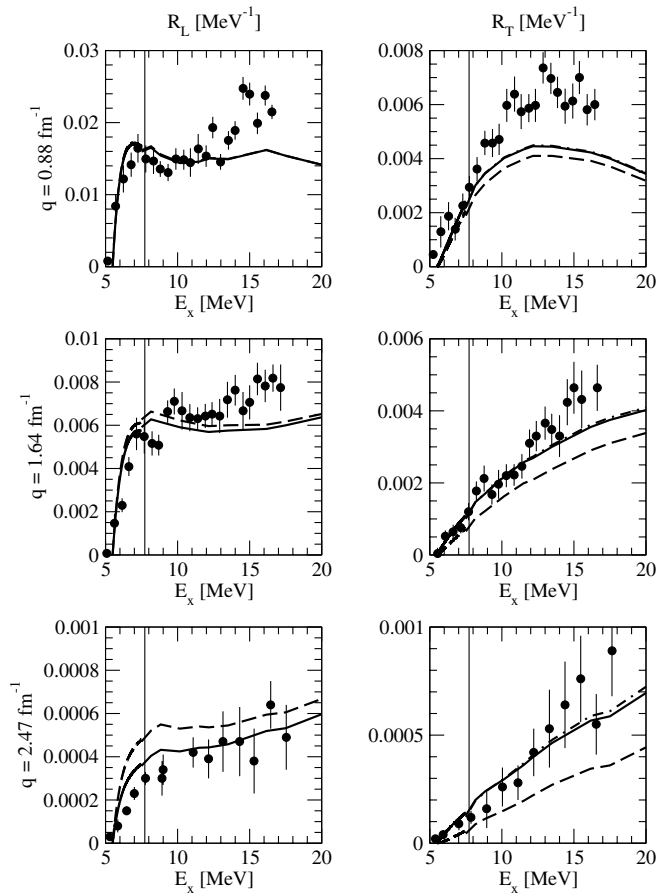


**Fig. 3.** Longitudinal and transverse response functions of  ${}^3\text{He}$ , obtained with the AV18/UIX Hamiltonian model. The experimental data are from [17]. The vertical line represents the  $ppn$  breakup threshold. See text for explanations of the different curves

which is an indication of the fact that if a Hamiltonian model with two- and three-nucleon interactions is used, then the model for the nuclear current operator should include the corresponding two- and three-body contributions.

The theoretical predictions for the longitudinal and transverse response functions  $R_L$  and  $R_T$  for  $q=0.88$ ,  $1.64$  and  $2.47 \text{ fm}^{-1}$  and  $5 \text{ MeV} \leq E_x \leq 20 \text{ MeV}$  are shown in Fig. 3. The vertical lines indicate the DBT. Although the calculation is extended above this threshold, no full three-body breakup channel is here included. The dashed, dotted-dashed and solid lines are obtained with only one-body current and charge operators, with the one- and two-body operators of [2], and with the one- and many-body transition operators presented in Sect. 2. Note that in the case of the charge operator, the model of [2] and the present one coincide. From inspection of the figure, we can observe that there is no significant difference between the results obtained using the model for the nuclear current operator of [2] and the present one. To draw any conclusion in the comparison between theory and experiment, a complete calculation which includes also the  $ppn$  channel should be performed.

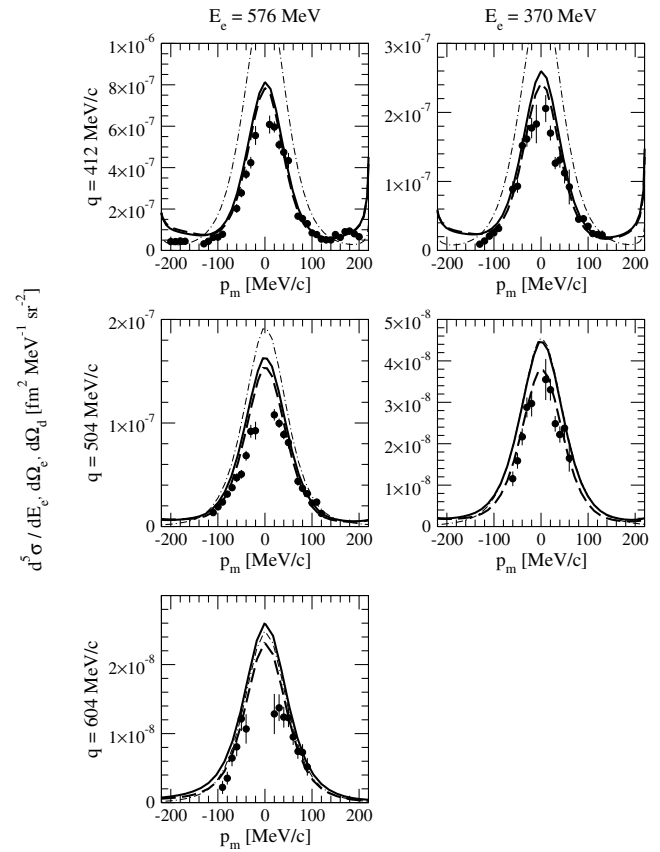


**Fig. 4.** Differential cross section of the  ${}^3\text{He}(e, e'd)p$  reaction obtained with the AV18/UIX Hamiltonian model as function of the missing momentum at three  $q$  values and two beam energies. The data are from [18]. See text for the explanation of the different curves

The theoretical predictions for the differential cross section of the  ${}^3\text{He}(e, e'd)p$  reaction as function of the missing momentum at beam energies of 370 and 576 MeV and  $q$  values of 412, 504 and 604 MeV/c are compared with the data of [18] in Fig. 4. The dotted-dashed lines correspond to the plane-wave impulse approximation results. When final-state-interaction effects are included and the  $pd$  final wave function is calculated with the PHH technique using the AV18/UIX Hamiltonian model, the dashed and the solid lines are obtained, depending if the one-body only or the one- and many-body contributions to the nuclear transition operators are retained. Here, no comparison is shown between the old model of [2] and the present one, since no significant differences have been seen. Note that this is the first calculation for the  ${}^3\text{He}(e, e'd)p$  reaction above DBT which uses the PHH technique to calculate the bound- and scattering-state wave functions including TNI and Coulomb force effects in the final-state interaction. By inspection of Fig. 4, we can conclude that there is an overall nice agreement between theory and experiment, although the data at low missing momentum are overestimated by the theory. This was already observed in [18], where the data were compared with a Faddeev calculation, with no Coulomb and three-nucleon interac-

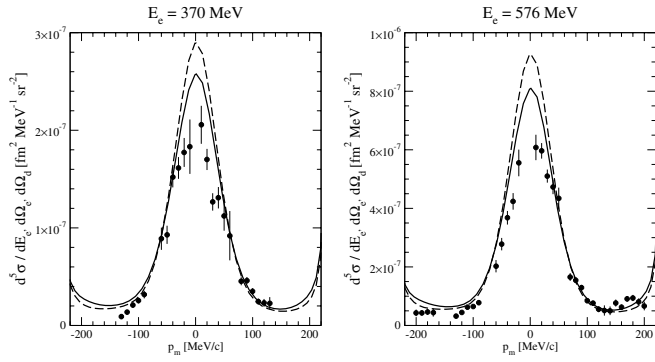


**Fig. 5.** Differential cross section of the  ${}^3\text{He}(e, e'd)p$  reaction as function of the missing momentum at  $q = 412$  MeV/c and beam energy of 370 MeV and 576 MeV. The *dashed* and *solid lines* correspond to the calculation performed with the AV18 and with the AV18/UIX Hamiltonian models, respectively. Data are from [18]

tion. However, we have verified that the inclusion of the UIX three-nucleon interaction improves the description of the data at zero missing momentum. This can be seen in Fig. 5, where the differential cross section at  $q = 412$  MeV/c and beam energy of 370 and 576 MeV is calculated with the AV18 (dashed curves) and the AV18/UIX (solid curves) Hamiltonian models. Only in this second case the model for the nuclear current operator includes three-body contributions, so that for each given Hamiltonian model the CCR is satisfied.

## 4 Summary and outlook

We have reported on new calculations of  ${}^3\text{He}(e, e')$  longitudinal and transverse response functions for three values of the momentum transfer and excitation energies from two-body threshold up to 20 MeV, and for  ${}^3\text{He}(e, e'd)p$  differential cross section as function of the missing momentum in  $(q, \omega)$ -constant kinematics, at two beam energies and three  $q$  values. These calculations use accurate bound and scattering state wave functions obtained with the PHH method from the Argonne  $v_{18}$  two-nucleon and Urbana IX three-nucleon interactions. The model for the electromagnetic charge operator includes one- and two-body components, while the model for the electromagnetic current operator includes one-, two- and three-body components, constructed so as to satisfy *exactly* the CCR with the given Hamiltonian model. The model for the nuclear current operator has been tested calculating the  $pd$  radiative capture cross section and spin observables. In particular, we have shown that the experimental  $T_{20}$  and  $T_{21}$  deuteron tensor observables are nicely reproduced by the present calculation. A systematic comparison between theory and experiment for the  $pd$  radiative capture in a wide range of  $E_{c.m.}$  is currently underway [9].

The  ${}^3\text{He}$  electrodisintegration observables here considered are very sensitive to the many-body contributions of the nuclear transition operators. However, no significant differences have been observed between the calcu-

lation performed with the present model of the nuclear current operator and the one of [2]. In the case of the  ${}^3\text{He}(e, e')$  reaction, no comparison can be done with the experimental data, since no  $ppn$  channel is included in the calculation. In the case of the  ${}^3\text{He}(e, e'd)p$  reaction, instead, the experimental differential cross section is fairly reproduced in the whole range of missing momentum for all different kinematics, when final-state interactions effects are considered. Further investigations for the  ${}^3\text{He}$  electrodisintegration in a wider energy range is vigorously being pursued.

*Acknowledgements.* The work of R.S. was supported by the U.S. DOE Contract No. DE-AC05-84ER40150, under which the Southeastern Universities Research Association (SURA) operates the Thomas Jefferson National Accelerator Facility.

## References

1. J. Carlson, R. Schiavilla: Rev. Mod. Phys. **70**, 743 (1998)
2. M. Viviani, A. Kievsky, L.E. Marcucci, S. Rosati, R. Schiavilla: Phys. Rev. C **61**, 064001 (2000)
3. A. Kievsky, M. Viviani, S. Rosati: Nucl. Phys. A **551**, 241 (1993); Nucl. Phys. A **577**, 511 (1994); A. Kievsky, S. Rosati, M. Viviani, Phys. Rev. C **64**, 024002 (2001)
4. R.B. Wiringa, V.G.J. Stoks, R. Schiavilla: Phys. Rev. C **51**, 38 (1995)
5. B.S. Pudliner, V.R. Pandharipande, J. Carlson, R.B. Wiringa: Phys. Rev. Lett. **74**, 4396 (1995)
6. D.O. Riska: Phys. Scr. **31**, 107 (1985); Phys. Scr. **31**, 471 (1985)
7. R. Schiavilla, D.O. Riska, V.R. Pandharipande: Phys. Rev. C **40**, 2294 (1989)
8. L.E. Marcucci, M. Viviani, A. Kievsky, S. Rosati, R. Schiavilla: Few-Body Syst. Suppl. **14**, 319 (2003); Few-Body Syst. Suppl. **15**, 87 (2003); M. Viviani, L.E. Marcucci, A. Kievsky, R. Schiavilla, S. Rosati: Eur. Phys. J. A **17**, 483 (2003)
9. L.E. Marcucci, M. Viviani, R. Schiavilla, A. Kievsky, S. Rosati: in preparation.
10. R. Schiavilla, D.O. Riska, V.R. Pandharipande: Phys. Rev. C **41**, 309 (1990)
11. L.E. Marcucci, D.O. Riska, R. Schiavilla: Phys. Rev. C **58**, 3069 (1998)
12. D.O. Riska: Phys. Rep. **181**, 207 (1989)
13. J. Carlson, D.O. Riska, R. Schiavilla, R.B. Wiringa: Phys. Rev. C **42**, 830 (1990)
14. R.G. Sachs: Phys. Rev. **74**, 433 (1948); E.M. Nyman: Nucl. Phys. B **1**, 535 (1967)
15. S.A. Coon et al.: Nucl. Phys. A **317**, 242 (1979)
16. M.R. Robilotta, M.P. Isidro Filho: Nucl. Phys. A **414**, 394 (1984); Nucl. Phys. A **451**, 581 (1986); M.R. Robilotta, M.P. Isidro Filho, H.T. Coelho, T.K. Das: Phys. Rev. C **31**, 646
17. G.A. Retzlaff et al.: Phys. Rev. C **49**, 1263 (1994)
18. C.M. Spaltro et al.: Nucl. Phys. A **706**, 403 (2002)
19. M.K. Smith, L.D. Knutson: Phys. Rev. Lett. **82**, 4591 (1999)
20. F. Goeckner, W.K. Pitts, L.D. Knutson: Phys. Rev. C **45**, R2536 (1992)